Numerical Simulation Study on the Influence of Cavity Behind Lining on Tunnel Structure Safety

Junbo Zhao*

Zijin School of Geology and Mining Fuzhou University Fuzhou, China

*Corresponding author: 162202223@fzu.edu.cn

Abstract. The total length of tunnels in China has ranked first in the world. However, in the construction of railway tunnels in difficult mountainous areas, it is easy to have cavity behind lining tunnel (CBLT) diseases. Moreover, in the operational tunnels, the proportion of CBLT diseases is also high. Therefore, the influence of CBLT on the safety of tunnel lining structure should be studied which is of great significance for ensuring safety and prolonging service life. Based on ABAQUS finite element analysis (FEA) software, the numerical models of CBLT are established respectively under four different working conditions: No CBLT, CBLT is on the arch bottom, arch top, spandrel. By comparing the displacement deformation characteristics, stress change characteristics and compression damage characteristics of the tunnel structure under these four working conditions, the law of the influence of cavity positions on the safety of the tunnel structure is obtained. Research results show that the influences of different positions of CBLT on the safety performance of lining structures are different. This research can be used to analyze the safety of tunnel structure in the presence of CBLT disease and guide the safety evaluation of tunnel..

Keywords: lining cavity, numerical simulation, tunnel safety.

1. Introduction

Between 2014 and 2024, as China's economy has been developing rapidly, the length of railway operation has exceeded 150,000 kilometers, and the length of high-speed railway opened to traffic has exceeded 40,000 kilometers. In China, 70% of which are mountains, hills and plateaus. The construction of large-scale railway infrastructure on these mountains and plateaus inevitably requires a large number of tunnels to connect [1]. By the end of 2023, 18,537 railway tunnels with a length of 23,508 km have been put into operation in China, and 2,668 with a length of 7,110 km are under construction [2].

Nowadays, the high-speed railway tunnel project has been moving towards the bad geological section of the difficult mountainous area in the west. However, the railway tunnels built in the difficult mountainous areas often have CBLT diseases due to poor construction quality control and untimely maintenance [3]. Tunnel construction is a complex system engineering, CBLT disease occurs frequently, in the current operation of the tunnel, the hole behind the lining disease accounts for about 25% [1].

Through literature review, the diseases of the lining of 3 tunnels are analyzed [1]. Huangtuling Tunnel (Pinggu District, Beijing, China) tunnel arch and side wall have many cracks accompanied by different degrees of water leakage disease, and there are CBLT at the development site of cracks and the spalling site of concrete. There are 15 CBLT in the left wall (Yunyang, Chongqing, China), 15 cavities on the top, 14 cavities in the arch bottom plate. There are more than 20 CBLT of Lijihuayuan Tunnel (Chongqing, China) with serious water leakage diseases [1].

As a common tunnel disease, lining crack damage is the result of long-term adverse effects of supporting structure and surrounding rock [4]. In China, the early construction of the tunnel generally adopts the form of straight wall, due to the uneven quality of tunnel construction, a large number of straight wall tunnel lining structure under the load variation and environmental effects of its long-term mechanical properties and durability is difficult to ensure, straight wall tunnel lining structure disease gradually emerged, it seems that the disease distribution phenomenon of straight wall tunnel lining structure is more serious. The CBLT is one of the primary factors contributing to lining

deterioration [5]. Consequently, an in-depth exploration of the impact of this CBLT on the safety of straight-wall tunnel structures is indispensable. Such research holds immense significance in guaranteeing the operational safety of straight-wall tunnels and enhancing their service life.

Zhang et al. studied the impact of cavities behind the lining on tunnels by establishing two-dimensional and three-dimensional (3D) FEA models. He concluded that the cavities at the arch top have a great influence on the tunnel structure [6]. Wang studied the bending moment and axial force of the lining structure in the presence of cavities in combination with the risk probability model in literature, and obtained a cavity risk assessment method [7]. In the study of Wang et al., a numerical simulation was adopted to obtain the laws of the influence of CBLT on the displacement and stress of the lining [8]. Che established a 3D FEA model to study the influence law of cavities behind the lining of straight-wall tunnels on the internal forces of the lining structure [9]. Zhu used ANSYS for numerical simulation analysis to study the mechanical properties of the lining structure under different stress fields and different cavities positions [10]. Liu used the numerical simulation calculation method to study the structural reliability indexes of the secondary lining structure under different conditions and different stress states [11]. Luo used the "Tongji Shuguang GeoFBA" FEA software to study the internal forces of the lining structure when there were CBLT and obtained the variation law of the internal forces [12]. Liu studied the influence of different characteristic parameters of cavities on the lining structure by establishing a numerical calculation model of tunnels containing cavities [13]. Lai et al. used the ANSYS FEA software to establish two-dimensional plane models with and without CBLT, studied the influence laws of cavities in terms of size and position on tunnels, and analyzed the variation laws of the bending moment and axial force [14].

According to the detection of geological radar, in fact, there are different degrees of holes in the lining arch, arch waist and other areas of highway tunnel [15]. Based on ABAQUS FEA software, this paper established four numerical models of CBLT under different working conditions, namely no CBLT, and the positions of CBLT are on the arch bottom, arch top and spandrel respectively. By comparing the deformation displacement, stress distribution characteristics of tunnel models under CBLT at different positions and the compression damage characteristics, the influence of CBLT on security was studied. To provide certain reference significance for tunnel structural safety evaluation.

2. Tunnel Lining Cavity Calculation Model

2.1. Model Establishment

Based on the ABAQUS FEA software, this chapter relies on the project of a two-way two-lane straight wall tunnel to establish a 3D model. The tunnel buried depth in the model is 300m. Fig. 1(a) is a cross-section of the tunnel. In the 3D model, about 4-5 times the tunnel diameter was taken on both sides of the tunnel, and the tunnel was taken from the surface upwards, limiting the horizontal x displacement of the model, the front and back z displacement, and the bottom y displacement. In order to fully consider the influence of the structural size limitations on the calculation and analysis of the structure, the geometric size of the model was selected as 40m×40m×10m. At the same time, the grid division should meet the requirements of calculation, and a total of 4055 grid units and 4788 nodes are divided. Fig. 1(b) shows the tunnel structure model after grid division.

2.2. Parameter Selection

In FEA, the surrounding rock meets the Moell-Coulomb constitutive relation and the lining is isotropic elastomer. When modeling the tunnel structure with CBLT disease, the V level surrounding rock is selected, surrounding rock arguments are selected by railway tunnel specifications. According to the design specification of tunnel support, it is also similar to other similar projects [16, 17]. The lining is set as a C20 concrete structure with a thickness of 40cm. The parameters of surrounding rock and lining structural materials selected in this paper are shown in Table I.

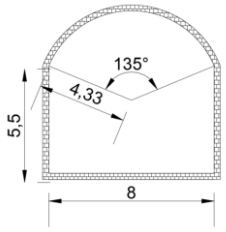

(a) Tunnel cross-section diagram.

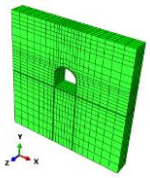

(b) Tunnel structure model diagram after grid division.

Figure 1. Tunnel structure and model diagram.

Table 1. Parameters Of Surrounding Rock And Lining Structure Materials

Type of material	Surrounding rock	Lining
Heavy gamma (kN/m^3)	20	25
Elastic module (Gpa)	1.5	20
Poisson's ratio	0.3	0.2
Cohesion (kPa)	150	/
Internal friction Angle (°)	25	/

2.3. Cavity Size and Shape Instructions

Previous studies have shown that CBLT of different shapes have limited influence on the force and deformation of tunnel structures. The mechanical characteristics and safety of lining structures basically cannot change with the change of CBLT shapes. Therefore, in order to simplify the analysis, in this chapter, CBLT are uniformly treated as rectangles when designing the model. The CBLT size is designed to be 3m long, 1m wide and 0.4m high. The schematic diagram of the CBLT is shown in Fig. 2.

Due to the different positions in which they appear, the CBLT are diverse. In order to simulate the CBLT disease in different positions and compare its influence on the stress of tunnel, four different numerical models of CBLT were established. The CBLT is located at the bottom of the arch, the top and the spandrel. In addition, for comparison, a tunnel structure model without CBLT is established. Therefore, there are four kinds of tunnel numerical models under different working conditions. The models with four working conditions are shown in Fig. 3.

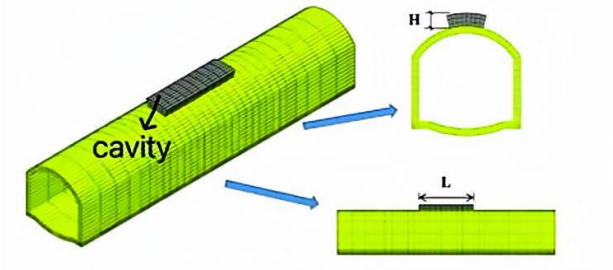

Figure 2. Schematic diagram of the cavity.

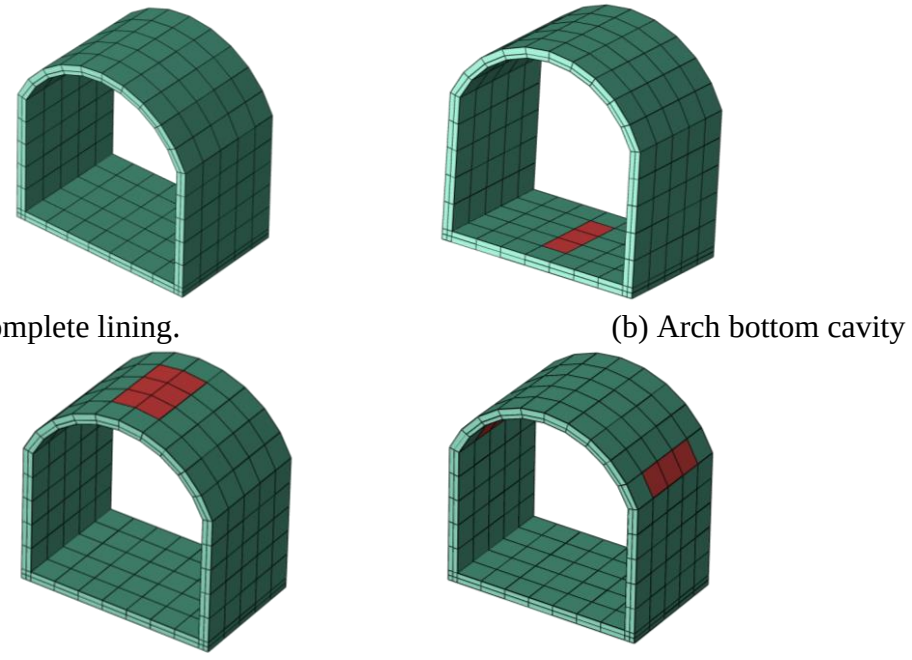

(a) Complete lining. (b) Arch bottom cavity

(c) Arch top cavity. (d) Spandrel cavity.

Figure 3. Four positions of CBLT.

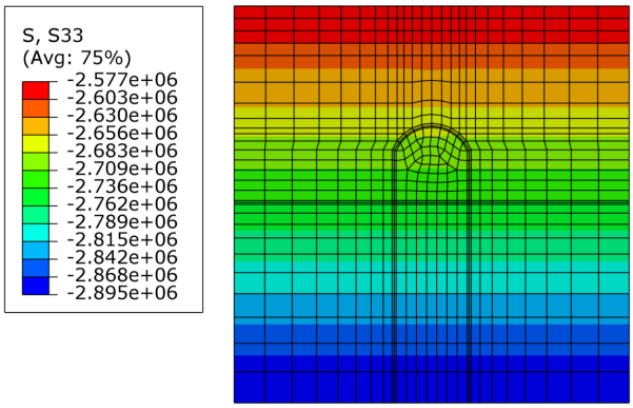

Figure 4. Initial geostress field.

2.4. Analysis Methods and Steps

Initial geostress balance: After the model is established, gravity is assigned to the model to simulate the initial geostress balance. After the balance is over, this part of the displacement is cleared to CBLT the impact on the calculation results. The initial geostress field is shown in Fig. 4

Rock mass excavation: In this calculation step, it is assumed that the tunnel is excavated by drilling and blasting method, and the stress release coefficient α=0.70 is taken according to similar projects. In this paper, the softening modulus method is used. The modulus of the rock mass in the excavation area is partially reduced before the lining construction to simulate the stress release effect during the excavation of the working face [18]. The ABAQUS model change function was used to activate the lining unit and kill the rock mass unit in the excavation area in two analysis steps.

Lining construction: In this step, the lining construction needs to be carried out in the initial stress ratio, that is, the original member is under a certain pressure, so the original structure has a certain deformation in the initial stress state, so the tracking element method (elcopy) is used to capture the deformation in the initial state.

3. Results and Discussion

3.1. Analysis of Displacement and Deformation

The deformation in displacement has the potential to impact both the stress levels and structural stability of the tunnel, potentially leading to significant secondary issues if the deformation becomes excessive. To precisely assess the influence of CBLT on the deformation of the surrounding rock and tunnel lining structure, it is imperative to examine the changes that occur in the cavity, surrounding rock, and lining structure during the tunnel's operational phase. This requires a thorough analysis of displacement and deformation. The numerical calculations related to displacement and deformation must also be verified. Fig. 5 depicts the cloud images for the maximum horizontal deformation displacement (MHDD) (left) and maximum vertical deformation displacement (MVDD) (right) of the tunnel lining under four operational scenarios. Table II summarizes the displacement and deformation conditions observed under these various scenarios. Additionally, Fig. 6 illustrates the maximum displacement curves for both horizontal and vertical displacements across the different operational conditions.

This phenomenon is particularly obvious when there is a CBLT in the spandrel. Since the position of MHDD and MVDD in this model almost does not change with the position of the CBLT (the MHDD appears in the side wall, and the MVDD appears on the top), this chapter compares the maximum displacement deformation value and the change of displacement and deformation at different positions of the cavity openings to reflect the deterioration performance of CBLT at different positions on the lining In Fig. 2 and Fig. 6, when there is a CBLT in the spandrel, the MHDD and MVDD of the lining are the largest among the four working conditions, and the horizontal displacement is 1.518mm respectively. The vertical displacement is 7.241mm, and the MHDD and MVDD increase by 11.7% and 7.5% compared with the complete lining condition. Moreover, the displacement and deformation increase at the spandrel cavity opening is much greater than that in other conditions, indicating that the spandrel cavity has the greatest influence on the displacement and deformation of the tunnel. In addition, it can be observed that except for spandrel CBLT, the displacement and deformation cloud images of the other three working conditions are symmetrical. In the case of spandrel CBLT, the maximum displacement and deformation of the side wall with CBLT increases significantly, which can also provide evidence for the deterioration of spandrel CBLT performance Finally, the vertical deformation displacement (VDD) is greater than the horizontal deformation displacement (HDD) under the four working conditions, indicating that the VDD has a stronger degradation effect on the lining structure performance than HDD.

Table 2. The Results of Maximum Displacement (mm)

CBLT position	MHDD		MVDD	
	Maximum	***Increment***	***Maximum***	***Increment***
Complete lining	1.358	/	4.874	/
Arch bottom	1.375	0.048	5.001	0.128
Arch top	1.385	0.463	4.863	0.012
Spandrel	1.497	0.364	4.965	1.420

3.2. Analysis of Stress Variation

When the CBLT disease appears, it will change the mechanical characteristics of the tunnel and surrounding rock, and break the original mechanical balance. In order to better grasp the mechanical characteristics of tunnel structure and lining structure, and understand the influence of CBLT on the force of tunnel structure and lining structure, it is necessary to extract the stress value in the model

calculation result for analysis [19]. Fig. 7 shows the maximum principal stress (MaxPS) nephogram (left) and minimum principal stress (Min PS) nephogram (right) of the tunnel lining under four working conditions.

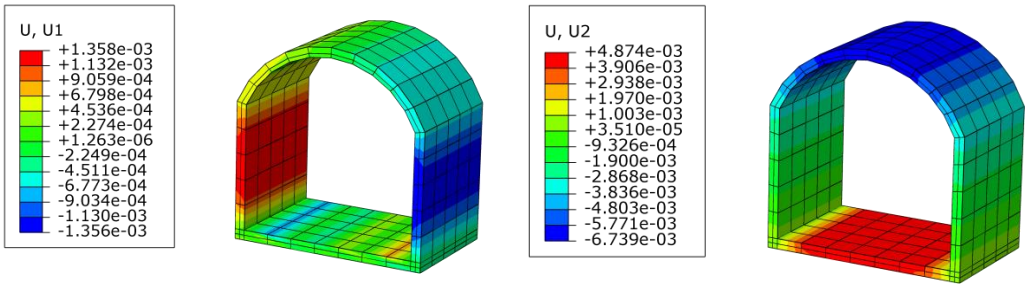

(a) Complete lining displacement nephogram.

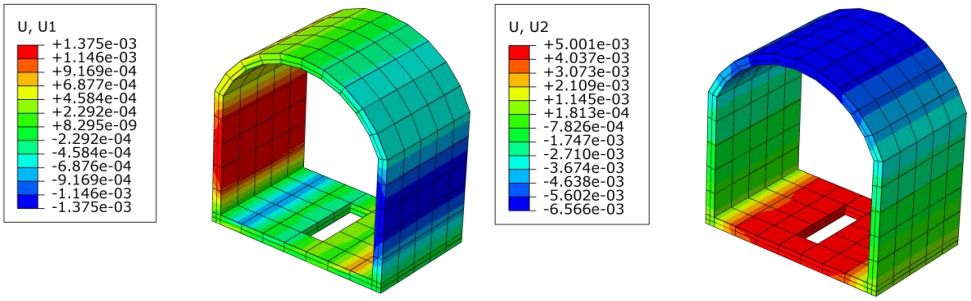

(b) Arch bottom cavity lining displacement nephogram.

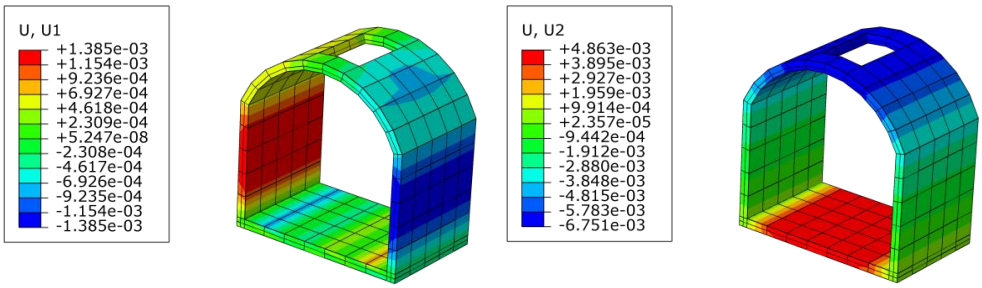

(c) Arch cavity lining displacement nephogram.

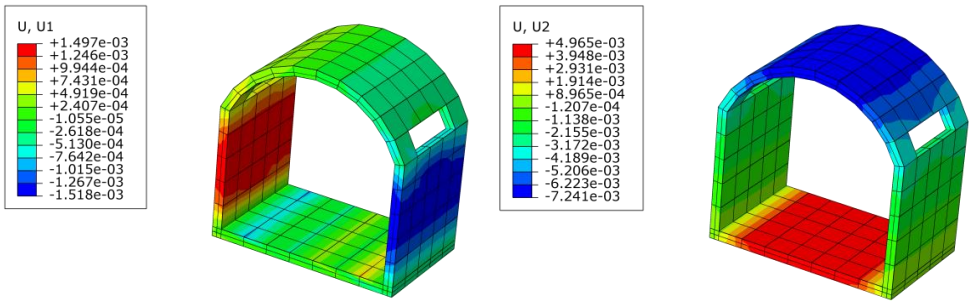

(d) Spandrel cavity lining displacement nephogram.

Figure 5. Tunnel lining displacement nephogram.

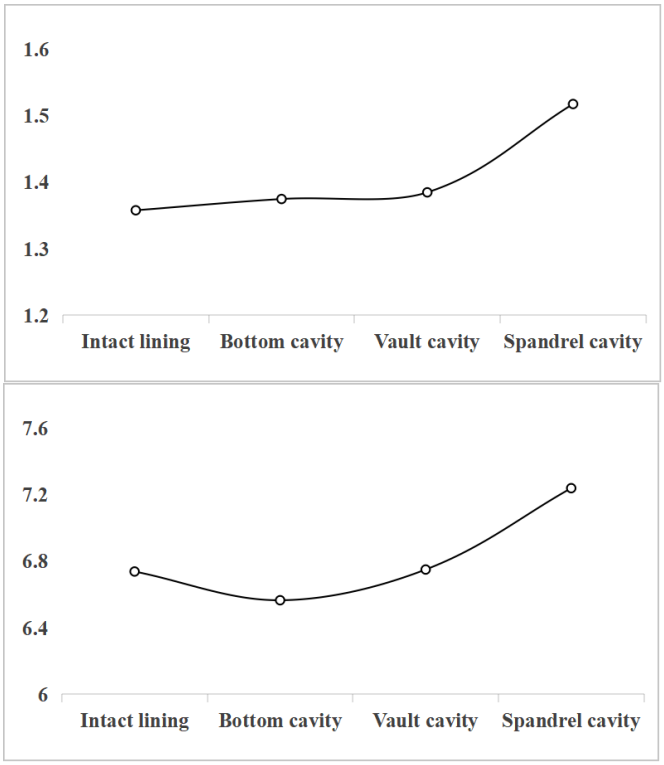

(a) Horizontal displacement. (b) Vertical displacement.

Figure 6. Curve of maximum displacement.

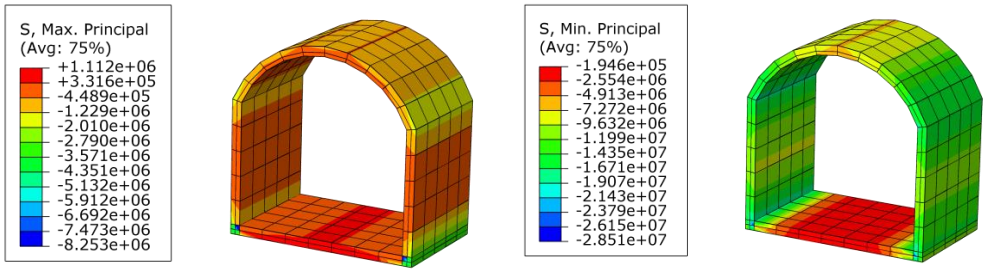

(a) Complete lining stress nephogram.

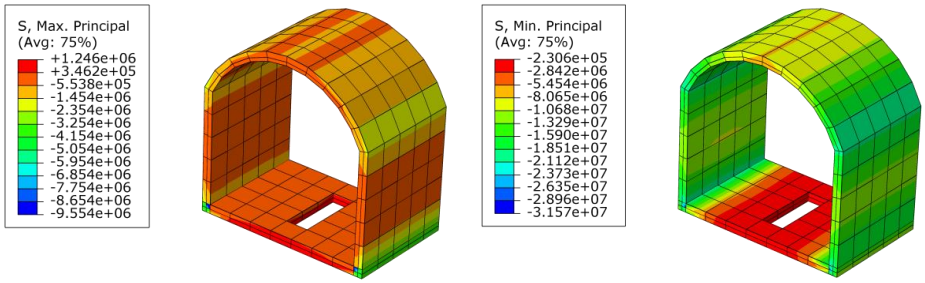

(b) Stress nephogram of arch bottom cavity lining.

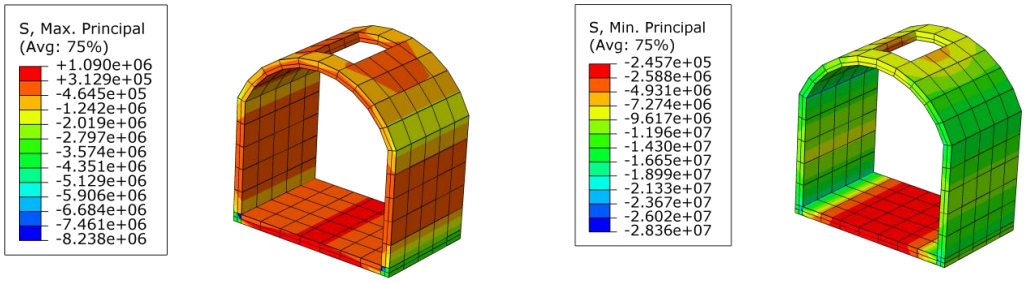

(c) Stress nephogram of arch cavity lining.

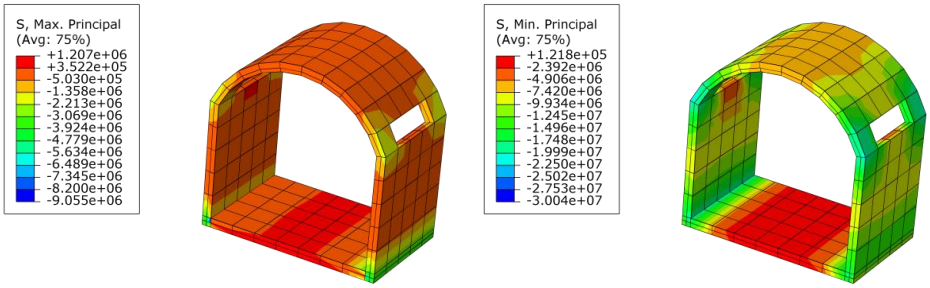

(d) Stress nephogram of spandrel cavity lining.

Figure 7. Stress nephogram of tunnel lining.

In the MaxPS nephogram, when there is no CBLT, the arch bottom tensile stress is the largest. When there is a CBLT at the bottom of the arch, the CBLT has a small influence on the lining, and the stress concentration at the CBLT is not obvious, but it has a great influence on the numerical value. When the CBLT appears on the top, the CBLT has a large influence on the lining, which mainly changes the stress state of the CBLT and the top lining. The stress concentration in the CBLT is more obvious, but the influence on the numerical value is small. When there is a CBLT in the spandrel, the CBLT has a large influence on the lining, mainly changing the stress state at the CBLT, the top and the bottom of the arch. The stress concentration at the CBLT is obvious, but the numerical influence is also small. It can be seen from the nephogram of minimum principal stress that when there is no CBLT, the maximum compressive stress appears at the arch bottom. When there is CBLT at the bottom of the arch, the change of lining stress is more obvious. Other changes are not obvious. When there is a CBLT on the top, the stress magnitude of the lining changes obviously. The stress distribution around the CBLT changes slightly, and the stress concentration in the CBLT is obvious. When there is a CBLT on the spandrel, the stress of the lining changes obviously, the stress distribution of the arch bottom, the top and the side wall changes obviously. The arch bottom changes from compressive stress to tensile stress. The stress concentration is obvious in the CBLT.

The MaxPS and MinPS of the lining and their positions are shown in Table III and Table IV when there are no CBLT and CBLT appear at each position. It can be seen from Table III and Table IV that the MaxPS occurs at the bottom of the arch, while the MinPS occurs near the bottom of the arch and the CBLT. The change of stress values is shown in Fig. 8. It can be seen from Fig. 8 that the MaxPS value is the largest when the CBLT is located at the arch bottom. When the CBLT is located at the arch top, the MinPS value is the largest.

Table 3. Variation of Maximum Principal Stress

CBLT position	MaxPS (Pa)	Position of the MaxPS	Stress change (Pa)
Complete lining	111200	Arch bottom	0
Arch bottom	124600	Arch bottom	13400
Arch top	109000	Arch bottom	-2200
Spandrel	120700	Arch bottom	9500

Table 4. Variation of Minimum Principal Stress

CBLT position	MinPS (Pa)	Position of the MinPS	Stress change (Pa)
Complete lining	-19460	Arch bottom	0
Arch bottom	-23060	Arch bottom	-3600
Arch top	-24570	Arch top, Spandrel	-5110
Spandrel	12180	Arch top, Spandrel	31640

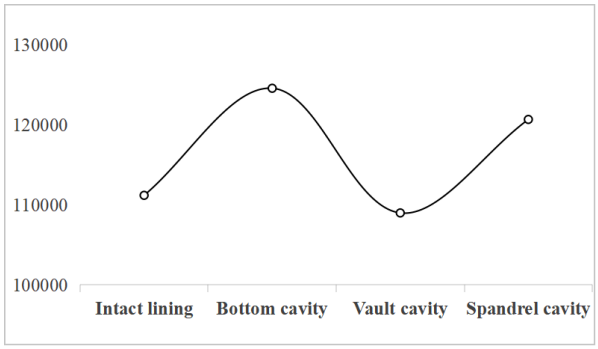

(a) Curve of maximum principal stress.

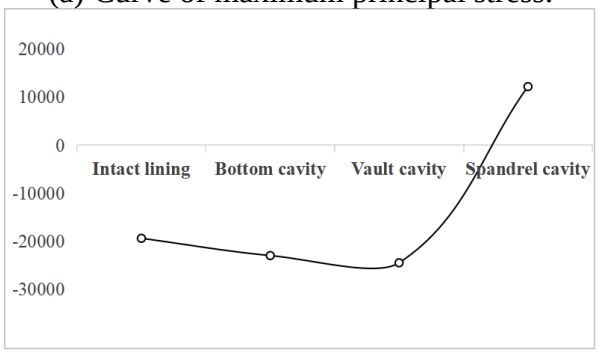

(b) Curve of minimum principal stress.

Figure 8. Maximum stress curve of tunnel lining.

3.3. Characteristics of lining compression damage

When CBLT appears, the mechanical properties of the lining will deteriorate. Moreover, deep-buried tunnels are under relatively high pressure. Therefore, exploring the influence of CBLT at different positions on the compression damage characteristics of the lining is the focus of this chapter. Through the study of the compression damage characteristics of different areas of the lining, the areas with greater lining damage can be identified, and these areas are regarded as dangerous areas. The above research can play a certain guiding role in tunnel construction and the reinforcement of tunnel operation in the future. The Concrete Damage Plasticity (CDP) model can take into account both the plastic deformation and damage effect of materials in the process of calculation. For the monotonic load analysis under the environment of low confining pressure and low strain rate, the compressive damage factor d_c (the value range of which is from 0 to 1, and the larger the value is, the greater the damage degree of the concrete material is. That is, when d_c= 0, indicates that the concrete is not damaged. When d_c = 1, it means the concrete material is completely damaged) is introduced to characterize the stiffness degradation degree of materials under tension and compression. Meanwhile, combined with the viscoelastic characteristics, the convergence of material calculation can be greatly improved [20]. In this chapter, the ABAQUS FEA software is adopted. Based on the CDP model, the compression damage characteristics of CBLT at different positions are analyzed. As shown in Fig. 9-12, they are the compression damage characteristics of the complete lining, the CBLT at the arch bottom, the CBLT at the arch top and the CBLT at the spandrel.

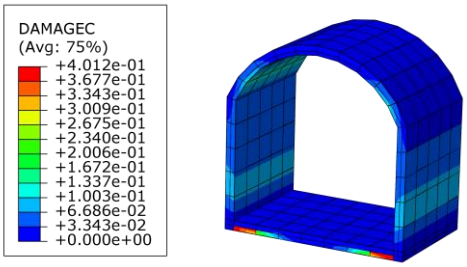

Figure 9. Characteristics of compressive damage of complete lining.

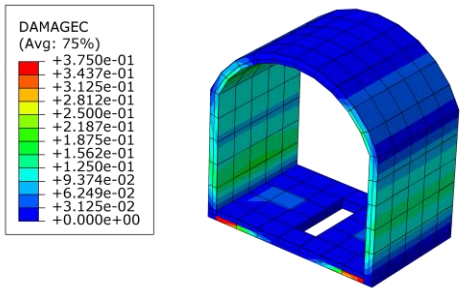

Figure 10. Characteristics of compressive damage of arch bottom cavity.

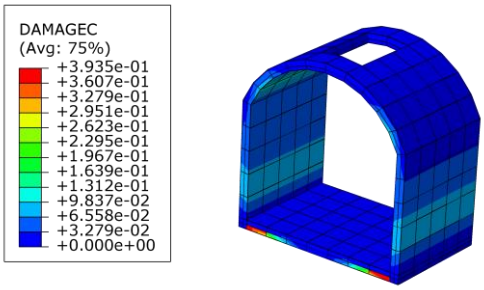

Figure 11. Characteristics of compressive damage of top cavity.

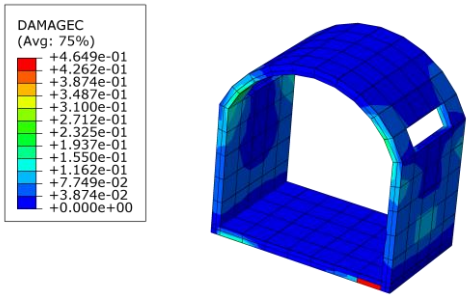

Figure 12. Characteristics of compression damage of spandrel cavity.

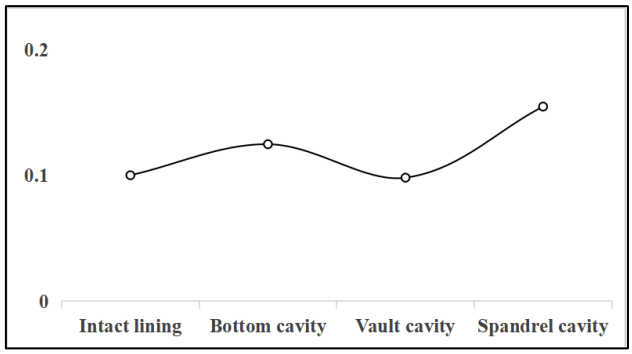

Figure 13. Maximum change curve of compression damage factor at the side wall.

It can be seen from Fig. 9-12, the compression damage characteristics of the lining that when cavities appear behind the tunnel lining, the compression damage characteristics of the lining will change. Although compared with the complete lining, the positions where the maximum damage factor values occur in the other three working conditions of CBLT remain unchanged, except for the situation where CBLT is located at the arch bottom, the characteristic positions of the lining's compression damage in the other two working conditions have changed significantly. In the working condition where CBLT is located at the arch bottom, the compression damage degree of the left and right side walls of the lining increases significantly, the compression damage degree at the spandrel increases slightly, and the maximum value of the damage factor decreases slightly. In the working condition where CBLT is located at the spandrel, the compression damage degree at the opening of the spandrel increases significantly, and the increasing characteristic generally reflects that the closer

to the opening, the higher the damage degree of the lining. Combined with the stress distribution characteristics in Section 3.2 of this chapter, it can be speculated that the increase in the compression damage degree at the opening is caused by the stress concentration at the opening. Moreover, in this working condition, the maximum value of the compression damage factor also changes greatly, increasing by 15.9% compared with the working condition of the complete lining.

In addition, by observing the four working conditions, it can be found that the lining with high compressive damage is mostly on the left and right side walls and both sides of the arch bottom. Since the volume of the areas with a high compression damage degree at the left and right side walls is relatively large, the maximum values of the compression damage factors at the left and right side walls under the four working conditions are compared to reflect the deterioration performance of the lining caused by CBLT at different positions. Among them, the curve of the change in the maximum value of the compression damage factor at the side wall under the four working conditions is shown in Fig. 13. It can be seen that when CBLT is located at the spandrel, it has the greatest impact on the safety of the lining. During the construction, maintenance and reinforcement processes, appropriate reinforcement should be carried out according to the actual situation to improve the overall stability of the surrounding rock mass.

4. Conclusion

Based on ABAQUS FEA software, numerical models of CBLT under different working conditions were established in this paper. By comparing the changes of deformation displacement, stress distribution, maximum and minimum principal stress and compression damage characteristics of tunnel models under different positions of lining cavities, the influence of CBLT on the tunnel safety was studied.

(1) In the four working conditions of complete lining, arch bottom cavity, top cavity and spandrel cavity, the horizontal displacement and vertical displacement of the lining are the largest when spandrel cavity appears, which indicates that spandrel cavity has the greatest influence on the displacement and deformation of the tunnel. Moreover, the VDD is greater than the HDD in all four working conditions, indicating that the vertical displacement has a greater impact on the structural performance of surrounding rock, while the HDD has a lesser impact on the structural performance of surrounding rock. When CBLT appears, in addition to the vertical displacement of the arch bottom cavity, the displacement and deformation around the hole will increase, indicating that CBLT at any position will have a certain deterioration effect on the lining performance

(2) Under the four working conditions, the positions where the MaxPS and MinPS of the lining occur remain almost unchanged, and they are all located at the arch bottom. When the CBLT appears at the arch top and spandrel, the stress concentration at the opening is obvious, and the stress distribution state undergoes relatively large changes. When the CBLT is located at the spandrel, not only is the stress concentration evident, the stress distribution state changes significantly, and the change in the stress value is also relatively large. It can be seen that when the CBLT is located at the spandrel, its effect on the stress characteristics of the lining is obvious. However, the CBLT at arch bottom has a relatively small impact on the stress distribution state. No obvious stress concentration is found at the opening either, and the change in stress is mainly reflected in relatively large numerical variations.

(3) Under the four working conditions, the linings with a high degree of compression damage are mostly located at the left and right side walls and on both sides of the bottom slab. When the Tunnel Backing Lining Cavity (CBLT) is located at the arch bottom, the volume of the lining suffering relatively large compression damage increases significantly, but the change in the compression damage factor is not obvious. When the CBLT is located at the arch top, neither the volume of the lining's compression damage nor the change in the compression damage factor is obvious. When the CBLT is located at the spandrel, the degree of compression damage at the opening increases significantly, and the compression damage factor at this position increases substantially, with an

increase rate of 54.5%. It can be seen that when the CBLT is located at the spandrel, the deterioration of the lining's safety performance is quite evident.

To sum up, whether comparing the displacement and deformation characteristics, stress characteristics or compression damage characteristics under the four working conditions, the Tunnel Backing Lining Cavity (CBLT) located at the spandrel will have a relatively large impact on the lining. It can be seen that compared with the CBLT at other positions, when the CBLT appears at the spandrel, the effect of deteriorating the safety of the lining is the most obvious. Therefore, special attention should be paid to this situation during the tunnel operation period.

References

[1] J.T. Xu, Lining Cavity, the Influence Law of Bearing Capacity of Tunnel Structure Research, Shijiazhuang: Shijiazhuang Railway University, June 2022.

[2] Gilian Technology, China Railway Tunnel Data Statistics in 2023, June 20th 2024. Retrieved on December 21. Retrieved from: https://c.aiiz.cn/jjSmfW.

[3] L. Yin, J. Zhu, W. Li, and J. Wang, "Vulnerability Analysis of Geographical Railway Network under Geological Hazard in China," ISPRS Int. J. Geo. Inf., vol. 9, pp. 342, June 2022.

[4] D.L. Zhang, "Basic problems and research progress of tunnels and underground engineering," Chin. J. Mech. Eng., vol. 49, pp. 3–21, November 2017.

[5] C. Liu, Study on Mechanical Characteristics of Tunnel Structure under Cavitation Condition at the Back of Arch Lining, Qingdao: Qingdao University of Technology, December 2018.

[6] S.L. Zhang, X.Q. Qi, C. Liu, D.G. Chen, "Highway tunnel lining cavity behind the distribution characteristics and its effect on lining structure," J. Build. Sci. Eng., vol. 37, pp. 62–70, March 2020.

[7] J.F. Wang. H.W. Huang. X.Y. Xie, Y.D. Xue, "Risk assessment of voids behind of the lings of mountain runnels", GeoFlorida 2010, pp. 2319-2328, 2012.

[8] J.F. Wang. H.W. Huang. X.Y. Xie and A. Bobet, "Void-induced liner deformation and stress redistribution," Tunn. Undergr. Space. Technol., vol.40, pp.263–276, May 2014.

[9] Z.J. Che, Study on the Influence of Cavitation in the Back of Straight Wall Tunnel Lining on Structural Safety, Qingdao: Qingdao University of Technology, August 2020.

[10] C.S. Zhu, X.H. Yang, H.P. Lai and Y.P. Zhu, "Influence of rear cavity on structural Safety of highway tunnel lining," J. Chang 'an Univ. (Natural Science Edition), vol.30, pp.63–68, September 2010.

[11] Y.H. Liu, Research on Safety Evaluation of Expressway Tunnel, Chengdu: Southwest Jiaotong University, 2004.

[12] X. Luo, Z.B. Li, J.Y. Zheng, "Research on voidness behind highway tunnel lining," Chinese Society of Civil Engineering, Tunnel and Underground Engineering Branch of Chinese Society of Civil Engineering, pp. 87–90, 2006 [Proceedings of the 12th Annual Meeting of the Chinese Society of Civil Engineering and the 14th Annual Meeting of the Tunnel and Underground Engineering Branch].

[13] H.J. Liu, C.C. Xia, Y.C. Cai, "Research and application of tunnel calculation model with cavity behind lining, Highway Tunnel," vol. 4, pp. 41–45, 2007.

[14] J.X. Lai, C. Liu, Z. Hu, X.J. Cao and X.L. Wang, "Numerical analysis of influence law of void behind shield tunnel lining on structure," Mod. Tunn. Technol., vol.54, pp. 126–134, June 2017.

[15] W.Y. Cui, J. Song, Y. Liu and Z.H. Yu, "Mechanical behavior analysis of tunnel lining caused by cavities at different positions," J. Water Res. Arch. Eng., vol.9, pp.70–73, October 2011.

[16] Chongqing Transportation Research and Design Institute. Code for Design of Highway Tunnel: JTGD70-2004. Beijing: People's Communications Press, 2004.

[17] General Institute of Architectural Research, Ministry of Metallurgy. Technical specification for bolt shotcrete support: GB 50086-2001. Beijing: China Planning Press, 2001.

[18] N. Boukpeti, D.J. White, "Interface shear box tests for assessing axial pipe-soil resistance," Géotechnique, vol.67, pp.18–30, January 2017.

[19] Y.Q. Wang, "Lining cavity influence law research about the safety of tunnel structure," Journal of western traffic science and technology, vol. 7, pp. 96–99, July 2023.

[20] J.W. Wang, L.X. Meng, M.L. Sun and E.X. Su, “Study on the effect of surrounding rock softening on the damage of tunnel secondary lining structure, ” Highway, vol.10, pp.443-449, October 2024.